tvst

Refractive Intervention

Predicting Implantable Collamer Lens Vault Using Machine Learning Based on Various Preoperative Biometric Factors

Yu Di[1,*], Huihui Fang[2,3,*], Yan Luo[1], Ying Li[1], and Yanwu Xu[2,3]

[1] Department of Ophthalmology, Peking Union Medical College Hospital, Chinese Academy of Medical Sciences, Beijing, China
[2] School of Future Technology, South China University of Technology, Guangzhou, China
[3] Pazhou Lab, Guangzhou, China

Correspondence: Yan Luo, Department of Ophthalmology, Peking Union Medical College Hospital, Chinese Academy of Medical Sciences, Beijing 100730, China. e-mail: lawyan@sina.com
Ying Li, Department of Ophthalmology, Peking Union Medical College Hospital, Chinese Academy of Medical Sciences, Beijing 100730, China. e-mail: liyingpumch@126.com
Yanwu Xu, School of Future Technology, South China University of Technology, Guangzhou 510641, China. e-mail: ywxu@ieee.org

Received: August 30, 2023
Accepted: December 6, 2023
Published: January 15, 2024

Keywords: ICL implantation; vault; random forest; XGBoost; linear regressor; machining learning

Citation: Di Y, Fang H, Luo Y, Li Y, Xu Y. Predicting implantable collamer lens vault using machine learning based on various preoperative biometric factors. Transl Vis Sci Technol. 2024;13(1):8, https://doi.org/10.1167/tvst.13.1.8

Purpose: To predict the vault size after Implantable Collamer Lens (ICL) V4c implantation using machine learning methods and to compare the predicted vault with the conventional manufacturer's nomogram.

Methods: This study included 707 patients (707 eyes) who underwent ICL V4c implantation at the Department of Ophthalmology, Peking Union Medical College Hospital, from September 2019 to January 2022. Random Forest Regression (RFR), XGBoost, and linear regression (LR) were used to predict the vault size 1 week after ICL V4c implantation. The mean absolute error (MAE), median absolute error (MedAE), root mean square error (RMSE), symmetric mean absolute percentage error (SMAPE), and Bland–Altman plot were utilized to compare the prediction performance of these machine learning methods.

Results: The dataset was divided into a training set of 180 patients (180 eyes) and a test set of 527 patients (527 eyes). XGBoost had the lowest prediction error, with mean MAE, RMSE, and SMAPE values of 121.70 µm, 148.87 µm, and 19.13%, respectively. The Bland–Altman plots of RFR and XGBoost showed better prediction consistency than LR. However, XGBoost showed narrower 95% limits of agreement (LoA) than RFR, ranging from −307.12 to 256.59 µm.

Conclusions: XGBoost demonstrated better predictive performance than RFR and LR, as it had the lowest prediction error and the narrowest 95% LoA. Machine learning may be applicable for vault prediction, and it might be helpful for reducing the complications and the secondary surgery rate.

Translational Relevance: Using the proposed machine learning model, surgeons can consider the postoperative vault to reduce the surgical complications.

Introduction

Myopia is the most common ocular disorder worldwide, with a prevalence of 10% to 30% in the adult populations of many countries.[1] Currently, there are several ways to correct myopia, such as spectacles, contact lenses, and refractive surgeries. However, high myopia and extremely high myopia (>−9.00 diopters [D]) corrections remain challenging due to refractive errors and corneal thickness.[2,3] The EVO ICL (Implantable Collamer Lens, model V4c; STAAR Surgical, Monrovia, CA) is a single-piece posterior chamber phakic intraocular lens designed with a

central hole. Since it became commercially available in 2011, it has been shown to be a safe and effective way to correct myopia.[4] Compared with conventional corneal refractive surgery, the correction range of ICL implantation is wide and does not involve limiting the corneal thickness. Therefore, it has been widely used in clinical practice, especially for the correction of high myopia and extremely high myopia.[5–7] The complications of ICL implantation are related to vault, which is defined as the distance between the anterior surface of the crystalline lens and the posterior surface of the ICL. The ideal vault ranges from 250 to 750 µm.[8] A low vault can lead to anterior subcapsular cataract,[9] whereas a high vault can lead to angle-closure glaucoma and pigment dispersion syndrome.[10] In these conditions, ICL alignment or replacement is necessary, but doing so could increase surgical risks and reduce patient satisfaction. Therefore, it is of great clinical significance to predict the vault after ICL implantation.

At present, some studies have used multiple linear regression analysis to establish ICL vault prediction formulas based on preoperative biometric factors.[11–15] However, due to the small sample sizes, the finesses of these prediction formulas were low ($R^2 < 0.41$). In addition, multiple linear regression analysis may ignore important nonlinear related parameters, which may reduce the accuracy of the prediction results. Therefore, a new method should be developed to predict the vault after ICL implantation. With the advancement of computational power, refinement of learning algorithms and architectures, and availability of big data, clinical deployment of artificial intelligence (AI) technology is now a promising reality in ophthalmology.[16] Machine learning, a subset of AI, is a powerful technique that identifies relationships among various variables and analyzes multidimensional data. This technique has been widely applied for the prediction of age-related macular degeneration,[17] classification of glaucoma,[18] and detection of keratoconus.[19] It might be a useful tool to predict the ICL vault; however, the related studies were limited, and the method could be further improved.[20,21] Enhanced preoperative parameters and unified vault prediction times are essential for machine learning model construction. Previous studies revealed that vault could remain relatively stable 1 week after ICL V4c implantation.[11,15] We found no vault-related complications at each follow-up time point when the vault was in the ideal range at 1 week after surgery in clinical practice. Therefore, the predicted vault in this study was determined to be 1 week.

The present study aimed to predict the vault using machine learning of preoperative parameters and to compare the predictive vaults with the conventional manufacturer's nomogram.

Methods

Patients

The study was retrospective in nature. Seven hundred and seven patients (98 men and 609 women; 707 eyes) who underwent ICL V4c implantation were recruited at the Peking Union Medical College Hospital (PUMCH) Department of Ophthalmology from September 2019 to January 2022. The inclusion criteria were as follows: (1) ages 18∼50 years; (2) spherical myopia up to −18.00 D and myopia astigmatism up to −6.00 D; (3) stable refraction for more than 2 years; (4) anterior chamber depth (ACD) ≥ 2.80 mm; (5) endothelial cell density ≥ 2000 cells/mm^2; (6) ICL V4c placed at 10° horizontally; and (7) vault size measured at 1 week after ICL V4c implantation. The exclusion criteria were as follows: (1) existence of ciliary body cysts; (2) existence of zonule abnormity; (3) existence of ocular diseases affecting vision, such as keratoconus, severe dry eye, active ocular infection, cataract, glaucoma, and fundus diseases that significantly affect vision; (4) existence of severe systemic diseases; and (5) loss of preoperative examination data (Fig. 1A). The conventional manufacturer's nomogram was used to select the ICL V4c size (12.1 mm, 12.6 mm, 13.2 mm, or 13.7 mm) based on white-to-white (WTW) distance and ACD. The study was approved by the PUMCH institutional review board (no. SK-2010) and was conducted in accordance with the tenets of the Declaration of Helsinki.

Surgical Procedures

All surgeries were performed by an experienced surgeon (LY). A 3.0-mm temporal corneal incision was made at the temporal corneoscleral limbus, and hyaluronic acid was injected into the anterior chamber. Then, an ICL V4c was inserted into the anterior chamber with an injector cartridge, and a positioning instrument was used to sweep the four haptics of the ICL beneath the iris. Subsequently, hyaluronic acid was completely removed from the eye using a manual irrigation/aspiration instrument. Ofloxacin eye ointment was administered, and sterile gauze was applied after confirming that intraocular pressure was normal. Patients were given antibiotic and steroidal medications 6 times daily for 3 days, and the dose was tapered thereafter.

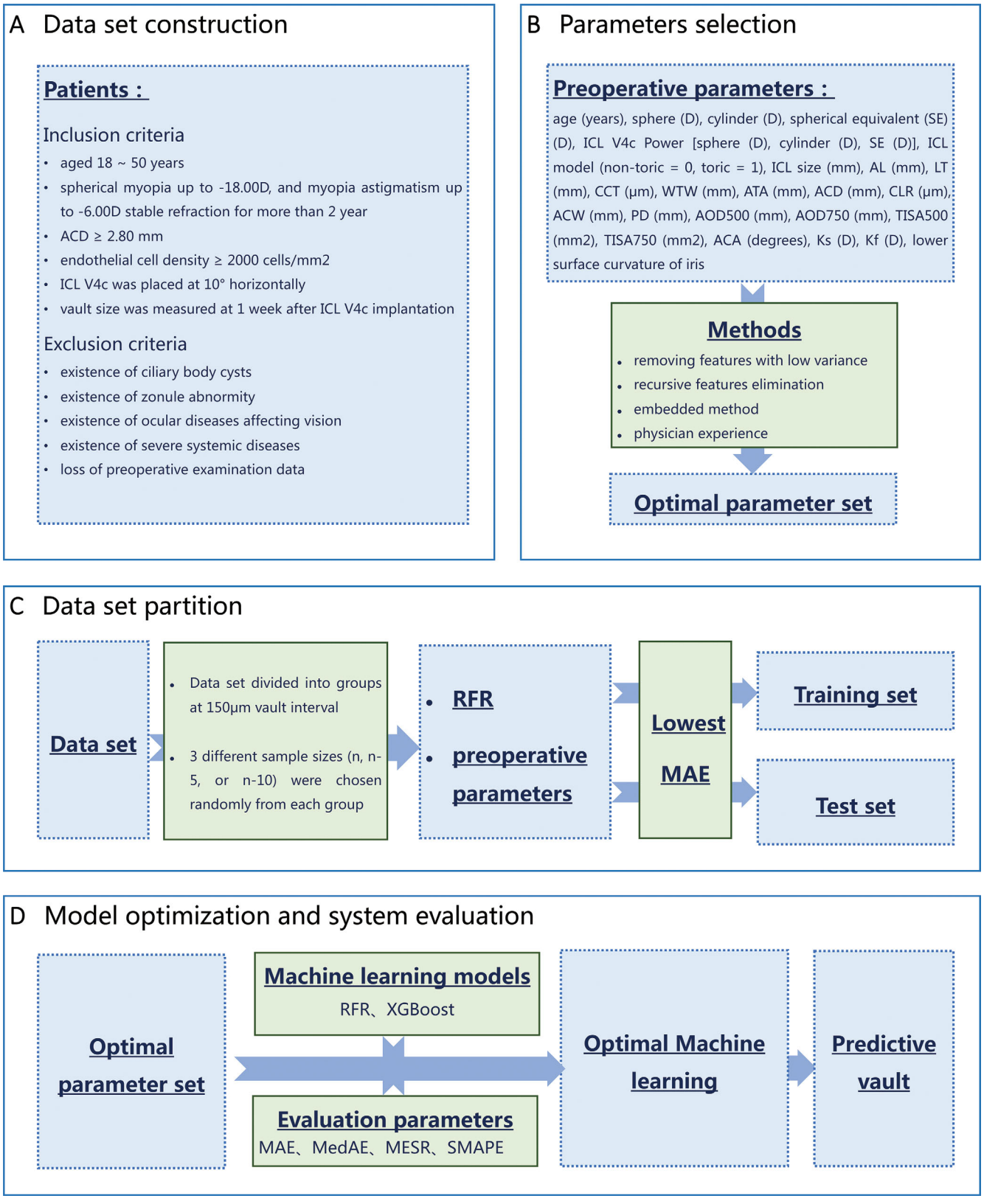

Figure 1. Workflow of constructing models.

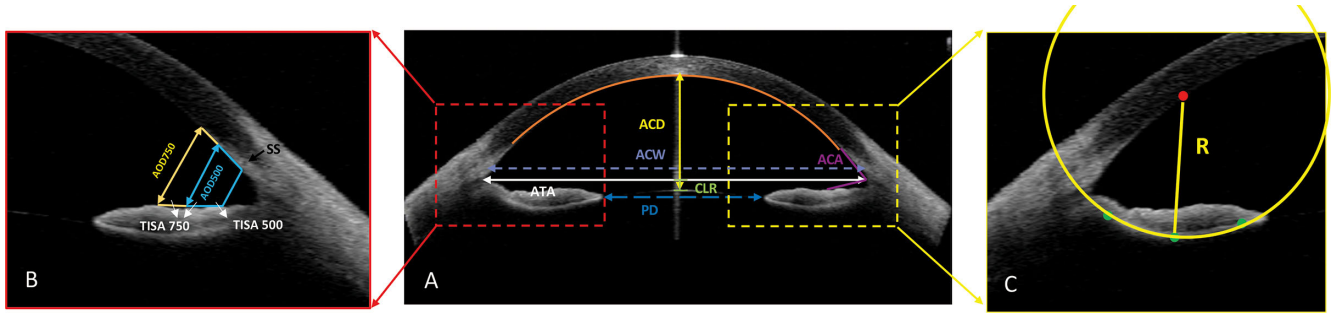

Figure 2. (**A**) ACD (mm) is the distance from the posterior surface of the central cornea to the anterior surface of the lens. The ACW (mm) is the distance between the scleral spurs. The ATA distance (mm) is the distance between the angle recesses. PD (mm) is the distance between the iris pupil margins. CLR (µm is the distance from the anterior surface of the crystalline lens to the ATA. (**B**) AOD500 and AOD700 indicate the angle opening distances at 500 µm and 700 µm, respectively. TISA500 and TISA700 indicate the trabecular iris space areas at 500 µm and 700 µm, respectively. (**C**) The inferior surface curvature of the iris is the lowest point; left and right ends of the lower surface of the iris were marked manually, and the curvature was calculated according to the formula $Cur = 1/R$ by fitting the above three points into a circle with radius R using an automatic algorithm.

Preoperative and Postoperative Measurements

Preoperatively, all patients underwent comprehensive ophthalmic examinations, including corrected distance visual acuity, intraocular pressure, anterior segment slit-lamp examination, fundus examination, and cycloplegic refraction. Corneal tomography (TMS-4; Tomey Corporation, Aichi, Japan) was used to measure the flattest meridian keratometry (Kf) and steepest meridian keratometry (Ks). Partial coherence interferometry (IOL Master 700; Carl Zeiss Meditec, Jena, Germany) was used to assess axial length (AL; mm), central corneal thickness (CCT; µm), WTW distance (mm), and lens thickness (LT; mm). Anterior segment optical coherence tomography (ASOCT, Visante; Carl Zeiss Meditec) was used to obtain ACD (mm), anterior chamber width (ACW; mm), angle-to angle (ATA) distance (mm), crystalline lens rise (CLR; µm), pupil distance (PD; mm), angle opening distance (AOD; 500 and 700 mm), trabecular iris space area (TISA; 500 and 700 mm^2), and anterior chamber angle (ACA) (Figs. 2A, 2B). The inferior surface curvature of the iris was obtained by PyQt5 framework development of annotation tools (Fig. 2C). Postoperatively, we measured the central vault at 1 week using the same ASOCT. The same examinations were performed by the same experienced physician under indoor natural light. Three measurements were taken for the average value.

Machine Learning Models of Preoperative Parameters

Regression models are applied to predict the vault, including Random Forest Regression (RFR), XGBoost, and linear regression (LR). The scikit-learn library (http://scikit-learn.org/stable/) for Python 3 was used. The input parameters were selected by removing features with low variance, recursive feature elimination, embedded methods, and physician experience. The scikit-learn library for Python 3 was used for the three former methods. The last method was based on physician experience and previous studies, which included the following parameters: spherical equivalent (SE; D), ICL V4c SE (D), ICL model (nontoric = 0, toric = 1), ICL size (mm), AL (mm), LT (mm), CCT (µm), WTW (mm), ATA (mm), ACD (mm), CLR (µm), ACW (mm), PD (mm), AOD500 (mm), AOD750 (mm), TISA500 (mm^2), TISA750 (mm^2), ACA (degrees), Ks (D) and axial, Kf (D) and axial, and inferior surface curvature of iris (Fig. 1B). Additionally, we applied the best performance model to identify the feature importance between the vault and preoperative parameters.

Dataset Partition

The dataset was divided into groups at 150-µm vault intervals, and three different sample sizes (n, $n - 5$, or $n - 10$) were chosen randomly from each group. We input all features and used RFR models to obtain the sample size of the training and test sets according to the lowest average mean absolute error (MAE) (Fig. 1C). Furthermore, we carried out random data partitioning three times and obtained datasets $R1$ to $R3$. Each dataset contained the same training and test samples.

Evaluation of Predictability Outcomes

The error between the predicted vault and the actual vault was evaluated by MAE, median

absolute error (MedAE), root mean square error (RMSE), and symmetric mean absolute percentage error (SMAPE) (Fig. 1D). The calculation formulas are provided in Supplementary Materials S1. Furthermore, the consistency between the predicted vault and the actual vault was evaluated by a Bland–Altman plot drawn by SPSSAU 22.0 (Qingsi Technology, Beijing, China). The differences in data are reported with 95% limits of agreement (LoA).

Statistical Analysis

The statistical analyses were conducted using SPSS Statistics 23.0 (IBM, Chicago, IL). The differences in MAE between machine learning methods were assessed using the Friedman test, and the Bonferroni test was employed for multiple comparisons. A two-tailed $P < 0.05$ was considered statistically significant for all analyses.

Results

Demographics of Patients

This study included 707 patients (707 eyes), with a mean age of 27.49 ± 5.75 years. A total of 472 eyes (66.76%) were implanted with a non-toric ICL V4c, and 235 eyes (33.24%) were implanted with a toric ICL V4c. The size of the implanted ICL V4c was 12.1 mm in 50 eyes (7.07%), 12.6 mm in 486 eyes (68.74%), 13.2 mm in 161 eyes (22.77%), and 13.7 mm in 10 eyes (1.41%). Table 1 lists the preoperative demographics and postoperative vaults of the patients.

Selection of Preoperative Parameters and Dataset Partition

Four methods were used to select the preoperative parameters, and physician experience showed the

Table 1. Preoperative Parameters and Postoperative Vault at 1 Week

Demographics	Mean ± SD	Range
Age (y)	27.49 ± 5.75	18∼45
Vault (mm)	0.66 ± 0.19	0.25∼1.31
Cycloplegic refraction (D)		
Sphere	−8.92 ± 2.97	−1.50∼−23.25
Cylinder	−1.40 ± 1.08	−6.75∼0.00
SE	−9.61 ± 3.12	−1.50∼−23.25
ICL V4c (D)		
Sphere	−10.85 ± 3.28	−2.50∼−18.00
Cylinder	0.77 ± 3.08	0.00∼5.00
SE	−10.52 ± 2.87	−2.50∼−18.00
Axial length (mm)	27.15 ± 1.43	23.06∼35.11
Lens thickness (mm)	3.70 ± 0.40	3.02∼4.64
Central corneal thickness (µm)	520.30 ± 34.51	422∼634
White-to-white distance (mm)	11.98 ± 0.51	10.70∼13.00
Angle-to-angle distance (mm)	11.71 ± 0.39	10.60∼13.09
Anterior chamber distance (mm)	3.24 ± 0.24	2.62∼4.03
Crystalline lens rise (µm)	−57.74 ± 169.24	−730∼520
Anterior chamber width (mm)	11.57 ± 0.39	10.37∼12.76
Pupil distance (mm)	4.88 ± 0.81	2.11∼6.85
Angle open distance, 500 mm	0.79 ± 0.26	0.28∼1.66
Angle open distance, 750 mm	1.04 ± 0.29	0.29∼1.91
Trabecular iris space area, 500 mm^2	0.28 ± 0.10	0.09∼0.67
Trabecular iris space area, 750 mm^2	0.51 ± 0.17	0.16∼1.09
Anterior chamber angle (°)	41.21 ± 8.07	19.75∼73.85
Flattest meridian keratometry (D)	44.48 ± 1.55	38.56∼49.44
Steepest meridian keratometry (D)	43.02 ± 1.41	34.00∼47.32
Lower surface curvature of iris	0.0022 ± 0.0050	−0.0100∼0.0019

Lower surface curvature of iris is the average value of the nasal and temporal values.

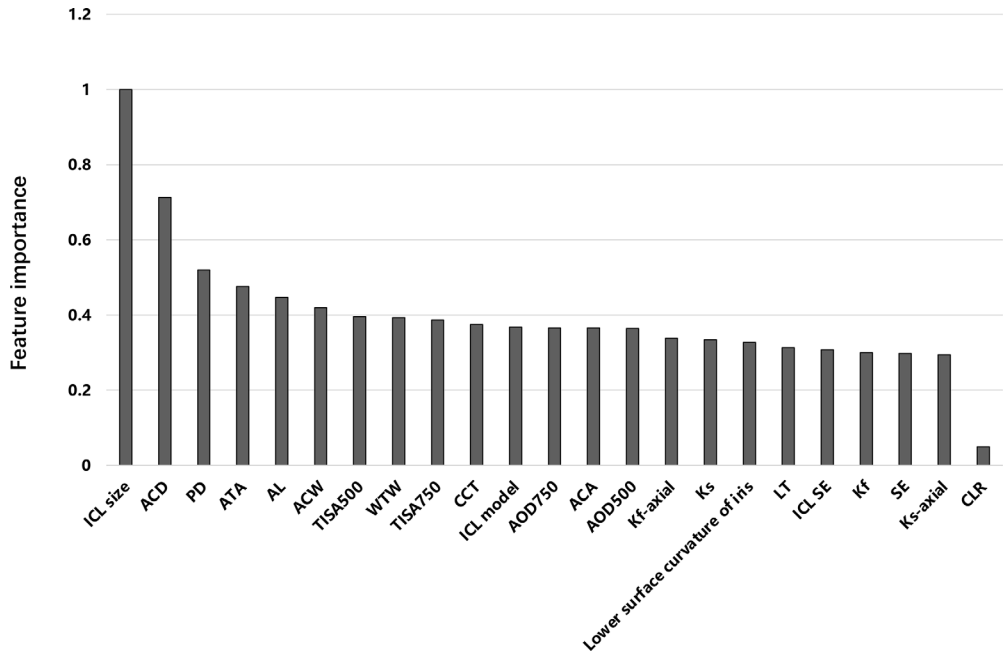

Figure 3. The highest importance aligned to 1.0 and scale the remaining values accordingly. ICL, implantable collamer lens; ACD, anterior chamber distance; PD, pupil distance; ATA, angle to angle; AL, axial length; ACW, anterior chamber width; TISA, trabecular iris space area; WTW, white to white; CCT, corneal central thickness; AOD, angle open distance; ACA, anterior chamber angle; Kf, flattest meridian keratometry; Ks, steepest meridian keratometry; LT, lens thickness; SE, spherical equivalent; CLR, crystalline lens rises.

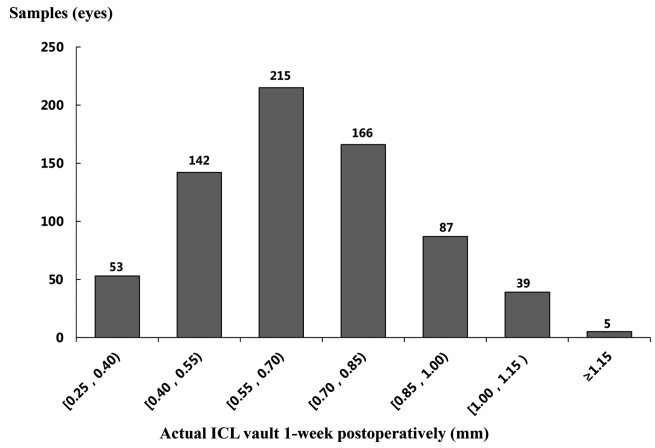

Figure 4. Distribution of the achieved implantable collamer lens (ICL) vault 1 week postoperatively.

lowest MAE value (119.79 µm) among these methods (Supplementary Material S2). Figure 3 compares feature importance among the vault and preoperative parameters. The ICL size was the most important parameter, followed by the ACD, PD, ATA, and AL. The 707 eyes were divided into seven groups at vault intervals of 150 µm (Fig. 4). The sample size of the group with vault more than 1.15 mm was small (five eyes). Thus, it was included in the test set to ensure the quality of model training. In the remaining six groups, the minimum sample size was 39 eyes. Groups were randomly chosen to include 30 eyes, 25 eyes, and 20 eyes for the training set, and the remaining eyes comprised the test set. The mean MAE values were 134.47 ± 0.48 µm, 137.05 ± 2.00 µm, and 138.36 ± 1.93 µm for each group of 30 eyes, 25 eyes, and 20 eyes selected, respectively. The lowest mean MAE value for each group of 30 eyes was selected; thus, sample sizes of 180 eyes in the training set and 527 eyes in the test set were determined. We carried out three random data partitions and obtained datasets *R*1 to *R*3. The ICL V4c size distributions in the *R*1 to *R*3 training sets were 12.1 mm for 10 eyes, 12.6 mm for 121 eyes, 13.2 mm for 46 eyes, and 13.7 mm for three eyes. In addition, 114 eyes were implanted with non-toric ICL V4c, and 66 eyes were implanted with toric ICL V4c.

Error and Consistency Evaluation of the Achieved Vault and Predictive Vault

The achieved ICL vault using the manufacturer's nomogram was 649.02 ± 103.95 µm, and the predicted ICL vaults using RFR, XGBoost, and LR were 675.47 ± 69.61 µm, 679.45 ± 71.75 µm, and 686.10 ± 114.27 µm, respectively. Table 2 shows the MAE, MedAE, RMSE, and SMAPE values for the predicted ICL vaults. For the MAE, XGBoost showed the lowest MAE, followed by RFR and LR. XGBoost showed

Table 2. Error Parameters of Various Machine Learning Methods for Vault Prediction at 1 Week Postoperatively

Error Parameters	Machine Learning Model	*R*1	*R*2	*R*3	Mean ± SD
MAE (µm)	RFR	129.28	120.33	119.79	123.13 ± 5.33
	XGBoost	125.58	120.24	119.29	121.70 ± 3.39
	LR	134.89	139.70	151.47	142.02 ± 8.53
MedAE (µm)	RFR	110.06	104.49	103.12	105.89 ± 3.68
	XGBoost	111.23	105.68	105.79	107.57 ± 3.17
	LR	112.00	115.82	117.79	115.20 ± 2.94
RMSE (µm)	RFR	159.83	149.01	148.59	152.48 ± 6.37
	XGBoost	153.23	147.51	145.87	148.87 ± 3.86
	LR	170.17	183.79	226.22	193.39 ± 29.23
SMAPE (%)	RFR	20.23	18.88	18.89	19.33 ± 0.78
	XGBoost	19.68	18.84	18.87	19.13 ± 0.48
	LR	20.95	21.75	20.43	21.04 ± 0.66

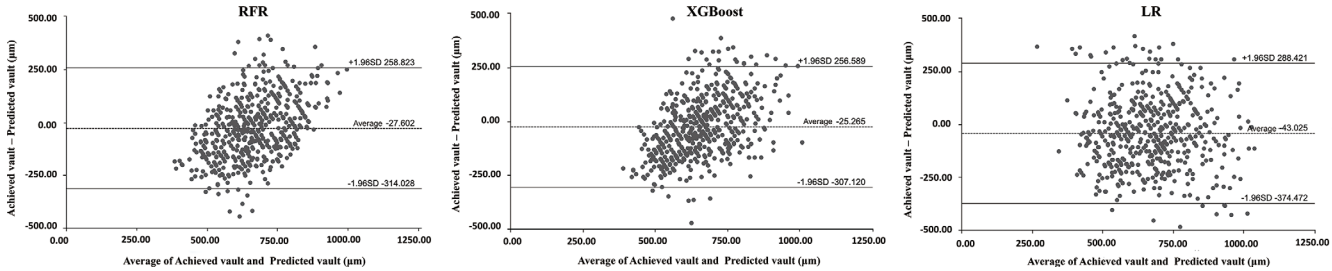

Figure 5. Bland-Altman plots of RFR, XGBoost, and LR. The *dotted lines* show mean differences between the achieved and predicted vaults; the *solid lines* are the upper and lower borders of the 95% LoA (mean difference ± (mean difference tlower the achieved and predicted vaultL) v).

significantly less MAE than LR ($P = 0.027$) but did not change from the RFR ($P = 0.064$). RFR demonstrated the lowest MedAE, followed by XGBoost and LR. However, XGBoost had the lowest RMSE and SMAPE, followed by RFR and LR. The Bland–Altman plots compared the consistency between the achieved vaults and predicted vaults using XGBoost, RFR, and LR (95% limits of agreement [LoA]). XGBoost demonstrated better consistency (−25.27 ± 143.81 µm; LoA, −307.12 to 256.59 µm) than RFR (−27.60 ± 146.138 µm; LoA, −314.03 to 258.82 µm) and LR (−41.13 ± 212.33 µm; LoA, −457.30 to 375.03 µm) (Fig. 5). In addition, for the MAE distribution of the predicted vaults, the percentages of eyes greater than 200 µm for XGBoost, RFR, and LR were 18.03%, 16.70%, and 26.19%, respectively.

Discussion

In the present study, we selected preoperative parameters by removing features with low variance, recursive feature elimination, embedded method, and physician experience. Then, RFR, XGBoost, and LR were trained to predict the vault at 1 week after ICL V4c implantation. MAE, MedAE, RMSE, and SMAPE were used to assess the error between the predicted vault and the actual vault. Furthermore, a Bland–Altman plot was used to evaluate the prediction consistency of these machine learning models. Our results demonstrated that XGBoost had the lowest prediction error, with mean MAE, RMSE, and SMAPE values of 121.70 µm, 148.87 µm, and 19.13%, respectively. The Bland–Altman plots of RFR and XGBoost showed better prediction consistency than LR. However, XGBoost showed narrower 95% LoA than RFR, ranging from −307.12 to 256.59 µm. This study proposed to evaluate the feasibility of using machine learning methods to predict the vault after ICL implantation, and XGBoost showed better performance than RFR and LR. It can not only reduce complications caused by too high or too low vaults but also reduce the secondary surgery rate.

Previous studies have shown that ICL V4c size, ICL V4c MRSE, ACD, ATA, ACW, CLR, LT, and PD are important parameters in predicting the vault after

ICL V4c implantation.[22–27] In our study, the physician experience selection method included the aforementioned parameters and showed the lowest MAE value (119.79 µm) among the four parameter selection methods. This result suggests that the best training quality of the model was obtained when applying parameters selected by this method as input. Furthermore, compared to previous machine learning models, our study included the inferior surface curvature of the iris measured by a self-developed program to indirectly reflect the iris morphological characteristics. Chen et al.[28] analyzed parameters associated with the vault after ICL V4c implantation and showed a 4% increase in the odds of a vault greater than 1000 µm for every 1° reduction in the iris–ciliary angle. The inferior surface curvature of the iris showed an opposite trend to changes in the iris–ciliary angle. This result indicates that a greater inferior surface curvature of the iris is associated with a higher probability of high vault after ICL V4c implantation. Shen et al.[21] compared the prediction results of different machine learning models and found that RFR had the best performance in predicting the vault after ICL V4c implantation. Our study also adopted RFR to predict the vault, but the RMSE was lower than that of the study by Shen et al.[21] We speculated that the difference in RMSE is related to the inferior iris surface curvature, which may improve the prediction performance of the model.

In 2018, Nakamura et al.[29] applied ASOCT to measure the anterior segmental parameters and used multiple linear regression analysis to establish an ICL vault size prediction formula, where ICL vault (mm) = 0.5 + 1.1 × (implanted ICL size – 4.575–0.688 × ACW [mm] – 0.388 × CLR [mm]). However, that study was based on few variables and a relatively small sample size. Therefore, Igarashi et al.[12] added preoperative parameters and obtained a different ICL vault size prediction formula: Ks formula (ICL vault [mm]) = 660.9 × (ICL size – ATA [mm] + 86.6). However, Ando et al.[30] performed a study to compare the achieved vault using a manufacturer's nomogram and the predicted vault using the KS formula. Their results showed that the predicted vault tended to overestimate the actual vault, especially when selecting a larger ICL size. This might be related to the ignorance of nonlinear factors associated with the postoperative vault. Compared to multiple linear regression analysis, RFR has superior performance because it does not have to consider issues related to the independence of variables, multicollinearity, and the normal distribution of residuals, and it can calculate the nonlinear effect between input variables.[31] Based on the findings of Kamiya et al.,[20] it was suggested that RFR performed better than LR in predicting the vault after ICL V4c implantation. Shen et al.[21] used various machine learning methods to predict the vault after ICL V4c implantation and found that RFR was the method with the best prediction. Our study also found that MAE, MedAE, RMSE, and SMAPE values of the RFR were lower than those of LR. Additionally, the 95% LoA of RFR were narrower than those of LR, indicating that the prediction performance of RFR is better than that of LR. It could be that the preoperative biometric variables may not exhibit a simple linear correlation with the postoperative vault, and LR has limitations in explaining the relationships between measurements. Thus, LR performance was inferior to that of RFR and XGBoost.[32]

XGBoost is a machine learning that could be used for both classification and regression.[33,34] Xu et al.[35] used XGBoost and RFR to predict subretinal fluid absorption at 1, 3, and 6 months after laser treatment in patients with central serous chorioretinopathy, and the results indicated that XGBoost had better performance than RFR in the external validation. The study revealed that XGBoost has the advantage of avoiding overfitting. Shen et al.[21] also found that XGBoost was more accurate than RFR in predicting the ICL V4c size at 12.1 mm. In our study, we found that XGBoost had a lower prediction error and narrower 95% LoA than RFR. Additionally, although RFR (136 cases) had a larger sample size of MAE within 50 to 200 µm than XGBoost (125 cases), RFR (95 cases) had a larger sample size of MAE above 200 µm than XGBoost (88 cases), which indirectly reduced the RFR prediction performance.

This study has several strengths. First, our study added anterior chamber angle parameters, developed annotation tools to obtain the inferior surface curvature of the iris, and controlled the direction of ICL V4c implantation. These measures could further improve the predictive performance of machine learning models. Second, XGBoost was used to predict the central vault at 1 week postoperatively, indicating the feasibility of this method in ophthalmic regression studies. However, this study also has limitations. First, our study performed only internal validation, but we will perform external validation in future studies. Second, the preoperative parameters of machine learning methods require manual input, which may lead to accidental errors. Third, our study had a large number of independent variables for the input parameters, and the sample size was not the largest compared to other studies.[20,21] Thus, in a future study, we would use some other machine learning methods to predict the postoperative vault. Finally, the ICL V4c size distribution in the samples was not balanced, which was related to the anterior segment characteristics of the

Chinese population. Thus, the sample size of patients implanted with the 13.7-mm and 12.1-mm ICL V4c was small, so the machine learning model may have better performance in predicting the postoperative vault after 12.6-mm and 13.2-mm ICL V4c implantation. We also found that the ICL V4c size had characteristics similar to those reported by Shen et al.,[21] whose study was related to the anterior segmental characteristics of the Chinese population.

Conclusions

In conclusion, we found that XGBoost has better predictive performance than RFR and LR, with the lowest prediction error and narrowest 95% LoA. These results support the view that machine learning is applicable for vault prediction, and it might be helpful for reducing the complications caused by a vault that is too high or too low, as well as for reducing the secondary surgery rate.

Acknowledgments

Disclosure: **Y. Di**, None; **H. Fang**, None; **Y. Luo**, None; **Y. Li**, None; **Y. Xu**, None

* YD and HF contributed equally to this work and both are the co-first authors.

References

1. Baird PN, Saw SM, Lanca C, et al. Myopia. *Nat Rev Dis Primers*. 2020;6(1):99.
2. Freeman CE, Evans BJ. Investigation of the causes of non-tolerance to optometric prescriptions for spectacles. *Ophthalmic Physiol Opt*. 2010;30(1):1–11.
3. Ang M, Gatinel D, Reinstein DZ, Mertens E, Alió Del Barrio JL, Alió JL. Refractive surgery beyond 2020. *Eye (Lond)*. 2021;35(2):362–382.
4. Kawamorita T, Shimizu K, Shoji N. Theoretical study on the need for laser iridotomy in an implantable collamer lens with a hole using computational fluid dynamics. *Eye (Lond)*. 2017;31(5):795–801.
5. Chen X, Wang X, Xu Y, et al. Five-year outcomes of EVO implantable collamer lens implantation for the correction of high myopia and super high myopia. *Eye Vis (Lond)*. 2021;8(1):40.
6. Lisa C, Naveiras M, Alfonso-Bartolozzi B, Belda-Salmerón L, Montés-Micó R, Alfonso JF. Posterior chamber collagen copolymer phakic intraocular lens with a central hole to correct myopia: one-year follow-up. *J Cataract Refract Surg*. 2015;41(6):1153–1159.
7. Sanders DR, Doney K, Poco M; ICL in Treatment of Myopia Study Group. United States Food and Drug Administration clinical trial of the Implantable Collamer Lens (ICL) for moderate to high myopia: three-year follow-up. *Ophthalmology*. 2004;111(9):1683–1692.
8. Alfonso JF, Lisa C, Palacios A, Fernandes P, González-Méijome JM, Montés-Micó R. Objective vs subjective vault measurement after myopic implantable collamer lens implantation. *Am J Ophthalmol*. 2009;147(6):978–983.e1.
9. Maeng H-S, Chung T-Y, Lee D-H, Chung E-S. Risk factor evaluation for cataract development in patients with low vaulting after phakic intraocular lens implantation. *J Cataract Refract Surg*. 2011;37(5):881–885.
10. Owaidhah O, Al-Ghadeer H. Bilateral cataract development and pupillary block glaucoma following implantable collamer lens. *J Curr Glaucoma Pract*. 2021;15(2):91–95.
11. Chen X, Miao H, Naidu RK, Wang X, Zhou X. Comparison of early changes in and factors affecting vault following posterior chamber phakic Implantable Collamer Lens implantation without and with a central hole (ICL V4 and ICL V4c). *BMC Ophthalmol.* 2016;16(1):161.
12. Igarashi A, Shimizu K, Kato S, Kamiya K. Predictability of the vault after posterior chamber phakic intraocular lens implantation using anterior segment optical coherence tomography. *J Cataract Refract Surg*. 2019;45(8):1099–1104.
13. Lee H, Kang DSY, Choi JY, et al. Analysis of pre-operative factors affecting range of optimal vaulting after implantation of 12.6-mm V4c implantable collamer lens in myopic eyes. *BMC Ophthalmol*. 2018;18(1):163.
14. Trancon AS, Manito SC, Sierra OT, Baptista AM, Serra PM. Determining vault size in implantable collamer lenses: preoperative anatomy and lens parameters. *J Cataract Refract Surg*. 2020;46(5):728–736.
15. Zhu Q-J, Chen W-J, Zhu W-J, et al. Short-term changes in and preoperative factors affecting vaulting after posterior chamber phakic Implantable Collamer Lens implantation. *BMC Ophthalmol*. 2021;21(1):199.

16. Murdoch TB, Detsky AS. The inevitable application of big data to health care. *JAMA*. 2013;309(13):1351–1352.
17. Thomas G, Grassi MA, Lee JR, et al. IDOCS: intelligent distributed ontology consensus system–the use of machine learning in retinal drusen phenotyping. *Invest Ophthalmol Vis Sci*. 2007;48(5):2278–2284.
18. Barella KA, Costa VP, Gonçalves Vidotti V, Silva FR, Dias M, Gomi ES. Glaucoma diagnostic accuracy of machine learning classifiers using retinal nerve fiber layer and optic nerve data from SD-OCT. *J Ophthalmol*. 2013;2013:789129.
19. Kovács I, Miháltz K, Kránitz K, et al. Accuracy of machine learning classifiers using bilateral data from a Scheimpflug camera for identifying eyes with preclinical signs of keratoconus. *J Cataract Refract Surg*. 2016;42(2):275–283.
20. Kamiya K, Ryu IH, Yoo TK, et al. Prediction of phakic intraocular lens vault using machine learning of anterior segment optical coherence tomography metrics. *Am J Ophthalmol*. 2021;226:90–99.
21. Shen Y, Wang L, Jian W, et al. Big-data and artificial-intelligence-assisted vault prediction and EVO-ICL size selection for myopia correction. *Br J Ophthalmol*. 2023;107(2):201–206.
22. Alfonso JF, Fernández-Vega L, Lisa C, Fernandes P, Jorge J, Montés-Micó R. Central vault after phakic intraocular lens implantation: correlation with anterior chamber depth, white-to-white distance, spherical equivalent, and patient age. *J Cataract Refract Surg*. 2012;38(1):46–53.
23. Chen X, Han T, Zhao W, et al. Effect of the difference between the white-to-white and sulcus-to-sulcus on vault and the related factors after ICL implantation. *Ophthalmol Ther*. 2021;10(4):947–955.
24. Kato S, Shimizu K, Igarashi A. Vault changes caused by light-induced pupil constriction and accommodation in eyes with an implantable collamer lens. *Cornea*. 2019;38(2):217–220.
25. Lee D-H, Choi S-H, Chung E-S, Chung T-Y. Correlation between preoperative biometry and posterior chamber phakic Visian Implantable Collamer Lens vaulting. *Ophthalmology*. 2012;119(2):272–277.
26. Nakamura T, Isogai N, Kojima T, Yoshida Y, Sugiyama Y. Optimization of implantable collamer lens sizing based on swept-source anterior segment optical coherence tomography. *J Cataract Refract Surg*. 2020;46(5):742–748.
27. Kojima T, Yokoyama S, Ito M, et al. Optimization of an implantable collamer lens sizing method using high-frequency ultrasound biomicroscopy. *Am J Ophthalmol*. 2012;153(4):632–637.e1.
28. Chen Q, Tan W, Lei X, et al. Clinical prediction of excessive vault after implantable collamer lens implantation using ciliary body morphology. *J Refract Surg*. 2020;36(6):380–387.
29. Nakamura T, Isogai N, Kojima T, Yoshida Y, Sugiyama Y. Implantable collamer lens sizing method based on swept-source anterior segment optical coherence tomography. *Am J Ophthalmol*. 2018;187:99–107.
30. Ando W, Kamiya K, Hayakawa H, Takahashi M, Shoji N. Comparison of phakic intraocular lens vault using conventional nomogram and prediction formulas. *J Clin Med*. 2020;9(12):4090.
31. Uddin S, Khan A, Hossain ME, Moni MA. Comparing different supervised machine learning algorithms for disease prediction. *BMC Med Inform Decis Mak*. 2019;19(1):281.
32. Chen X, Ye Y, Huan Yao, et al. Predicting postoperative vault and optimal implantable collamer lens size using machine learning based on various ophthalmic device combinations. *Biomed Eng Online*. 2023;22(1):59.
33. Yoo TK, Ryu IH, Choi H, et al. Explainable machine learning approach as a tool to understand factors used to select the refractive surgery technique on the expert level. *Transl Vis Sci Technol*. 2020;9(2):8.
34. Yang C, Liu Q, Guo H, et al. Usefulness of machine learning for identification of referable diabetic retinopathy in a large-scale population-based study. *Front Med (Lausanne)*. 2021;8:773881.
35. Xu F, Xiang Y, Wan C, et al. Predicting subretinal fluid absorption with machine learning in patients with central serous chorioretinopathy. *Ann Transl Med*. 2021;9(3):242.